Title
Shear-wave splitting analysis of a 3d vsp from the san juan basin

Authors
Maultzsch, S.
Liu, E.
Li, X.-Y.
et al.

Publication Date
2003-05-01

Z-99 SHEAR-WAVE SPLITTING ANALYSIS OF A 3D VSP FROM THE SAN JUAN BASIN

S. MAULTZSCH[1], E. LIU[1], X.-Y. LI[1], T.M. DALEY[2], J.H. QUEEN[3], D. COX[3]

[1]*Edinburgh Anisotropy Project, British Geological Survey, Murchison House, West Mains Road, Edinburgh EH9 3LA, UK*

[2]*Lawrence Berkeley National Laboratory*

[3]*Conoco Inc.*

Summary

A quantitative characterization of fracture properties in naturally fractured tight gas reservoirs is of great importance for understanding reservoir properties. This study presents the analysis of a 3D-VSP data set from the San Juan Basin with regard to shear-wave anisotropy. The results indicate heterogeneity in the fracture distribution at the reservoir level. Overall, the time delays between split shear waves at reservoir depths are relatively small. This may be due to the presence of several fracture orientations in the target.

Introduction

As part of a USDOE funded project, a 3D VSP has been recently acquired in the San Juan Basin in northern New Mexico. The aim of the project is to quantify fracture properties in a tight gas reservoir in order to identify fractures that control permeability. The problem is approached by analysing data at different frequency ranges (borehole data to surface seismic), which are sensitive to scale-dependent effects (Majer *et al.*, 2002).

This study aims to further quantify the length scale of fractures from analysis of the multi-component 3D VSP data. Our hypothesis is that frequency dependent anisotropic effects can be used to deduce an average fracture size from seismic data. This concept is based on a previous study from a tight gas reservoir in the Uinta basin, where we could successfully discriminate between the effects of fractures at a metre scale and micro-cracks from multi-component VSP data (Maultzsch *et al*., 2003).

53 source locations were chosen to acquire the 9-C VSP data in the San Juan Basin. Two different shear-wave sources (IVI and IO) were used for comparison. 3-C receivers were placed at depths between 1200 ft and 5150 ft with a 50 ft or 25 ft spacing. The reservoir zone (Mesa Verde Group) is located below 4000 ft. Here we present the initial analysis of the data for shear-wave anisotropy using results of estimating polarization directions and time delays between split shear waves from direct arrivals. The information is used to gain insight into fracture orientations and intensity at the target.

Data processing and results

A rotation analysis was performed on 4-C shear-wave data in order to obtain the polarization directions of split shear waves. We used the linear transform technique (Li and Crampin, 1993), which allows for an independent rotation of source and geophone, and it resolves non-orthogonal shear waves.

Figure 1 shows the 4-C data from shot point 1000 before and after rotation. The rotation aims to minimize the energy in the cross-diagonal components (XY and YX), the results of which can be seen on the right in Fig. 1. The polarization angles are obtained from the rotation angle, while the time delays between the split shear-waves are computed by a cross-correlation analysis of the rotated data. In the presence of one dominant vertical fracture set, the polarization of the fast shear wave indicates the orientation of the fractures while the time delay is a measure of fracture intensity.

Where shear-wave splitting could be observed, inspection of the results for all shot points reveals relatively small time delays at the reservoir level (< 5 ms over 1000 ft). Figure 2 shows a map of the source locations and the VSP well. The orientation of the lines through the shot points indicates the azimuth of the fast shear-wave polarization, while their length is proportional to the time delay measured over the reservoir interval (length at loc. 91 corresponds to 1 ms). There is a dominant NE – SW trend in the polarization of the fast shear wave, although there is some variation with source location. The time delays estimated from near-offset data vary between 0 and 4 ms, while far offsets show larger time delays (sources 166 and 187).

Figure 3 shows the polarization angle (measured clockwise from the source-well axis) and the time delay obtained for source location 1000. There is a clear change of polarization direction with depth. The time delay increases strongly in the overburden, reaching 15 ms at a depth of 2500 ft. It then increases again by a few milliseconds at the reservoir level below 4000 ft.

The results for shot point 177 are plotted in Figure 4. Here the time delay increases steadily with depth, but the total amount of time delay is relatively small. The polarization angles show a large scatter at shallow depths.

The data from source location 1007, which is southwest of the well, revealed no shear-wave splitting at the target (no increase in time delay). But large shear-wave anisotropy in the overburden (Fig. 5) is detected. The time delay increases up to 15 ms at 2200 ft.

The last example (Fig. 6) shows the results for a far-offset shot location. There is a significant increase in time delay at the reservoir level. The incidence angles for the data above 3000 ft exceed 45º. Therefore, this portion of the data does not fall into the shear-wave window, where split shear-waves are polarized orthogonal and along the symmetry axes of the medium.

Discussion

Overall, the results of the shear-wave splitting analysis indicate heterogeneity in the fracture distribution within the target interval. A dominant NE - SW orientation of polarization angles was found, which agrees with the strike direction of major faults in the area and results from DSI logs. However, the corresponding time delays are very small, and for several locations the shear-wave anisotropy in the overburden is much larger than in the target interval. The low shear-wave anisotropy could be due to the presence of several fracture sets with different orientations. A comparison of production data with P-wave anisotropy derived from 3D seismic showed little correlation, which supports the same hypothesis (Majer et al., 2002).

The analysis of P-wave traveltimes and attenuation are initiatives of future work. Modelling and analysis of frequency-dependent anisotropic effects, which is based upon a new poroelastic model derived by Chapman *et al.* (2002), will include the influence of multiple fracture sets at different orientations.

Acknowledgements

This work was supported by the sponsors of the Edinburgh Anisotropy Project. It is published with the approval of the Executive Director of the British Geological Survey (NERC).

References

Chapman, M, Zatsepin, S.V. and Crampin, S., 2002: Derivation of a microstructural poroelastic model. Geophysical Journal International. **151**, 427-451.

Li, X. -Y. and Crampin, S., 1993, Linear-transform techniques for processing shear-wave anisotropy in four-component seismic data: Geophysics, Soc. of Expl. Geophys., **58,** 240-256.

Majer, E.L., Queen, J.H., Daley, T.M., Murphy, J., Fortuna, M., Lynn, H., Coates, R., Eike, P., Sinton, J., Cox, D., Myer, L., Nihei, K. and Nakagowa, S., 2002, Scaling between logs, single well, VSP and surface seismic for fracture quantification in naturally fractured gas reservoirs: 72nd Internat. Ann. Meeting, Salt Lake City, Soc. of Expl. Geophys., Expanded Abstracts.

Maultzsch, S., Chapman, M. and Liu, E., 2003, The potential of estimating fracture sizes from the frequency dependence of anisotropy: EAGE 65th Internat. Conference, Stavanger, Expanded Abstracts.

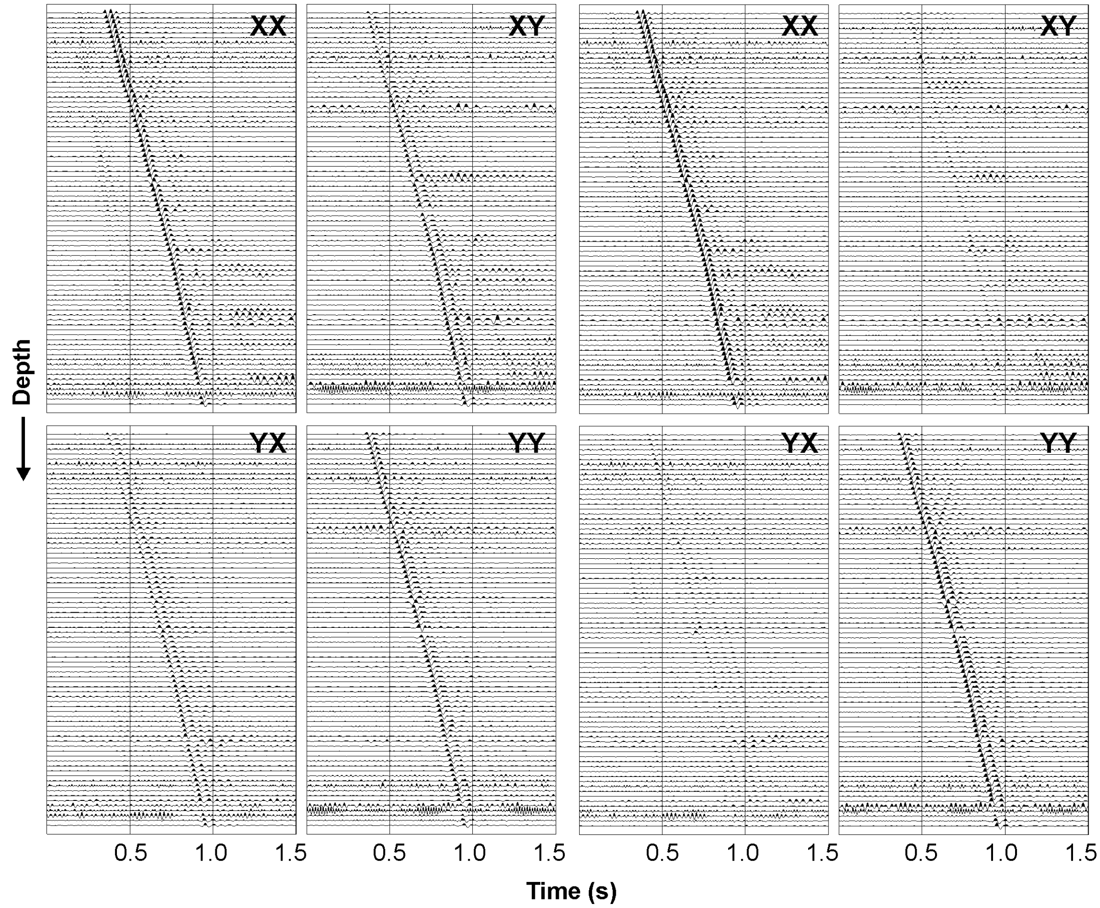

Fig. 1: 4C-VSP data from source location 1000 before (left) and after rotation (right). The rotation minimizes the energy in the cross-diagonal components.

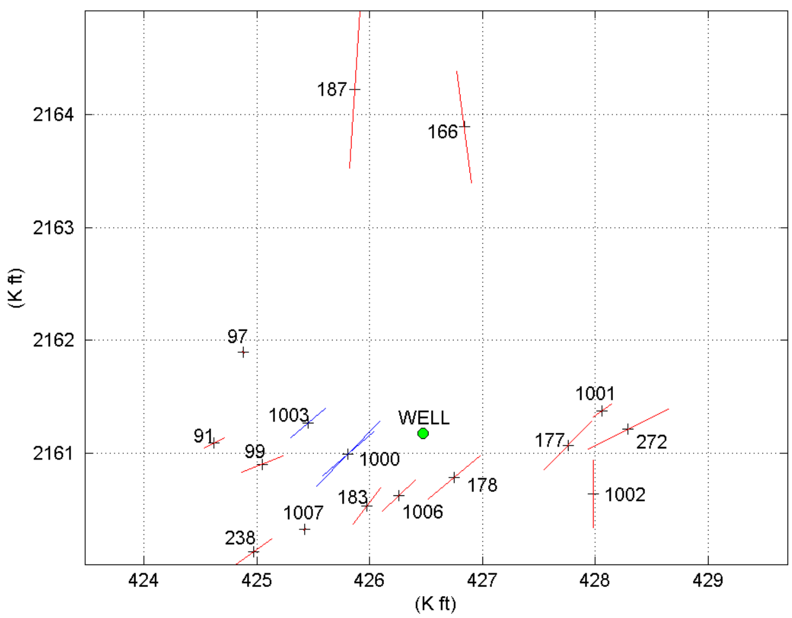

Fig. 2: Map of source locations, the VSP well and results of shear-wave splitting analysis. The direction of the lines through the source points indicates the azimuth of the polarization of the fast shear wave. The length of the lines is proportional to the time delay between the split shear waves over the reservoir interval with the shortest length corresponding to 1 ms. There is a general NE-SW trend in polarization angles, but the time delay at reservoir level is relatively low for most locations.

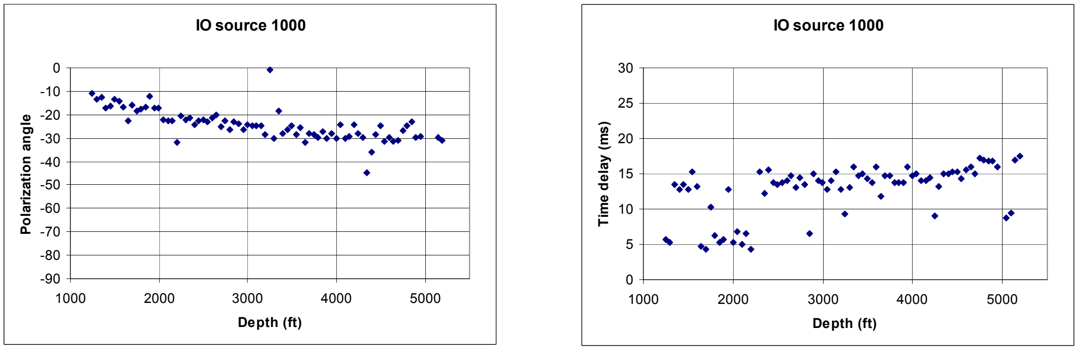

Fig. 3: Polarization angle (measured clockwise from the source-well axis) and time delay for source location 1000. There is strong shear-wave anisotropy in the overburden, while the time delay increases only slightly over the reservoir interval. The polarization angles change with depth.

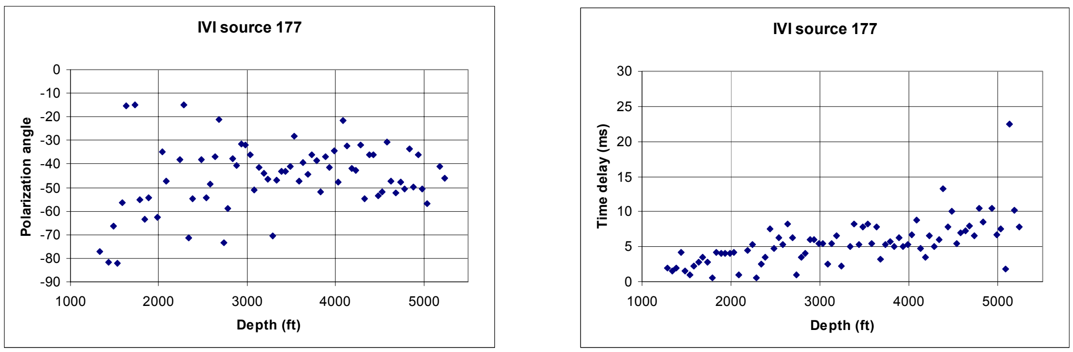

Fig. 4: Results for source location 177 show a slight steady increase of time delay with depth. The polarization angles show a large scatter at shallow depths.

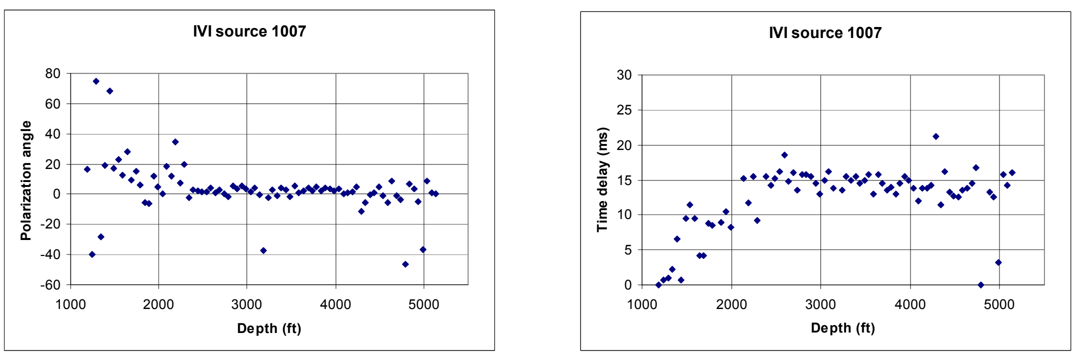

Fig. 5: Results for source location 1007 demonstrate large shear-wave anisotropy in the overburden, while no shear-wave splitting can be observed in the target interval.

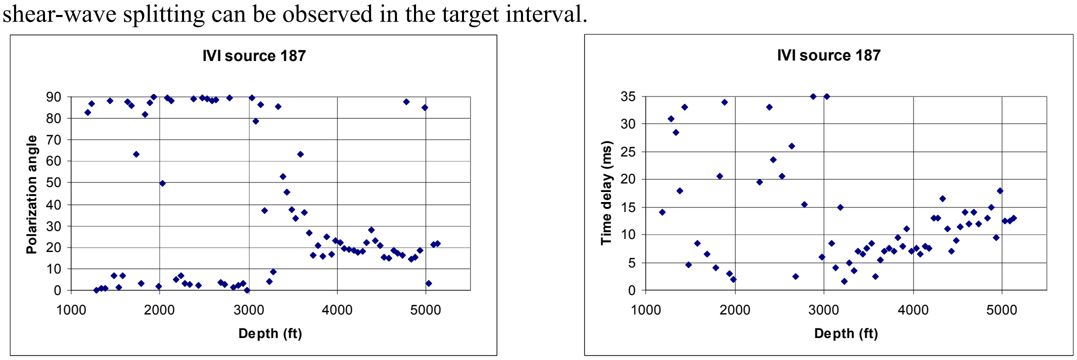

Fig. 6: The data from the far-offset location 187 show a large increase in time delay over the reservoir interval.